Estimating Temporal Parameters of Wheelchair Propulsion based on Hand Acceleration

Journal:	*RESNA 2008 Annual Conference*
Manuscript ID:	draft
Submission Type:	Student Scientific Paper
Date Submitted by the Author:	n/a
Complete List of Authors:	Hiremath, Shivayogi; University of Pittsburgh, Rehabilitation Science and Technology Ding, Dan; University of Pittsburgh, Rehabilitation Science and Technology Koontz, Alicia; University of Pittsburgh, Rehabilitation Science and Technology
Topic Area:	Mobility (M)

Estimating Temporal Parameters of Wheelchair Propulsion based on Hand Acceleration

Shivayogi Hiremath, BS, Dan Ding, PhD, Alicia Koontz, PhD
Department of Rehabilitation Science and Technology, University of Pittsburgh
5044 Forbes Tower, Pittsburgh, PA 15260
Human Engineering Research Laboratories, VA Pittsburgh Healthcare System, Pittsburgh, PA

ABSTRACT
Studies investigating wheelchair propulsion biomechanics usually utilize a SMARTWheel to quantify propulsion stroke frequency, an important risk factor for upper-extremity repetitive strain injury and/or pain. The aim of this paper was to estimate temporal parameters of wheelchair propulsion including stroke frequency, propulsion time, and recovery time based on hand acceleration. Twenty-nine manual wheelchair users propelled over linoleum and carpet while kinetic and kinematic data were collected. Estimates of the temporal parameters based on the three-dimensional hand acceleration were compared with those based on the SMARTWheel. The results revealed intraclass correlation coefficients (ICC) of 0.938, 0.815, 0.753 over linoleum and 0.994, 0.962, 0.901 over the carpet for the stroke time, the propulsion time, and the recovery time, respectively. Using hand acceleration to determine temporal parameters of wheelchair propulsion offers the possibility to quantify wheelchair propulsion performance and upper limb usage in community living conditions with accelerometry-based activity monitors.

KEYWORDS
Wheelchair Propulsion, Acceleration, Cadence, Biomechanics

BACKGROUND
Manual wheelchair propulsion is one of the important daily living activities involving repetitive usage of upper limbs among wheelchair users. A number of studies in ergonomics have strongly implicated the frequency of task completion as a risk factor for repetitive strain injury and/or pain at the wrists and shoulder (1, 2). Boninger et al. found that propelling with lower stroke frequencies may keep wheelchair users from developing median nerve injuries. Spending more time on the pushrim allows for forces to be distributed over a longer distance which could potentially minimize high impact forces to the upper limbs (3). Previous studies utilized vision systems and devices like a SMART^{Wheel} (Three Rivers Holdings Inc., Mesa, AZ) to detect the propulsion phase and the recovery phase of a stroke and determine stroke frequencies (i.e., cadence). The cost and intricate setting of the vision systems and SMART^{Wheel} have limited their use within research laboratories and rehabilitation clinics. The propulsion repetitiveness and the quality of upper limb movements that occur on a daily basis need to be investigated.

An accelerometry-based activity monitor has shown to be a valid instrument to quantify different types of mobility-related activities (4). Postma et al. found that wheelchair propulsion can be validly detected from a series of representative daily life activities by accelerometry-based activity monitors in patients with SCI (4). However, studies that use activity monitors to estimate specific propulsion biomechanical variables are missing. Jung-Ah et al. showed that an accelerometry-based activity monitor is a reliable and valid tool for identification of temporal gait parameters such as stance, swing, single support and double support time of gait cycles (5).

The first aim of this study was to estimate temporal parameters of wheelchair propulsion such as stroke frequency, propulsion time, and recovery time based on hand acceleration of the 3MP. A secondary aim was to compare the estimated temporal parameters to the same parameters determined by the SMART^{Wheel} to evaluate the accuracy of this new method.

METHODOLOGY

Experimental Protocol: The data for this study was collected during the National Veteran Wheelchair Games in Minneapolis, MN in 2005. Manual wheelchair users who owned a wheelchair and had no prior history of upper limb fractures or dislocations that they have not recovered from were recruited in the study. A six-camera *VICON MX* motion analysis system (Vicon, Centennial, Co) aligned on the left side of the wheelchair user was used to capture the position of the third metacarpalphalangeal joint (3MP) and the rear axle of his/her manual wheelchair at 60Hz. A SMART^{Wheel} (Three River Holdings, Inc. Mesa, AZ) attached on the left side of the subject's wheelchair collected pushrim forces and moments at 240 Hz. It can also detect the time instances of propulsion and recovery phases as well as the stroke frequency. Subjects were asked to propel their own wheelchairs on two surfaces including level linoleum and high-pile carpet. The linoleum remnant was 4' by 15'and the carpet remnant was 5' by 15'. Each surface was completed in a random order. Subjects were asked to propel at a comfortable pace for three times on each surface starting from rest. The VICON system and Smart^{Wheel} were synchronized to collect kinematic and kinetic propulsion data over the entire surface.

Estimation Algorithm: The hub position was subtracted from the position of the 3MP in order to create propulsion pattern plots (Figure 1). The three-dimensional acceleration at the 3MP in the direction of motion (x-axis), lateral direction (y-axis), and direction against gravity (z-axis) was calculated as shown in equation 1 (6). The first two start-up strokes from each trial were omitted and the rest of the strokes ranging from strokes 3 to 5 were averaged in the analysis.

Figure 1 and Equation 1 Go Here

The SMART^{Wheel} data was down-sampled from 240 Hz to 60 Hz and used to identify when the hand was on and off the pushrim to determine the time instances of each propulsion and recovery phase. This method served as a reference. Estimation algorithms based on 3MP acceleration were developed to obtain such time instances as well and compared with the reference method. During the propulsion phase, the hand traces the arc of the pushrim, thereby traveling away from the axle hub resulting in positive velocities in the x-axis. During the recovery phase, the hand travels towards the rear of the wheelchair opposing the motion of the wheelchair resulting in negative velocities in the x-axis. Such velocity transitions from positive to negative due to the change from propulsion phase to recovery phase result in negative discernable transient acceleration signals in the x-axis, indicating the start of a recovery phase. A computer program written in Matlab (Mathworks Inc.) first detected the maximum negative acceleration in the x-axis, and based on the maximum value a band of 60% to 100% of the maximum value was created where other local negative peak accelerations were identified. The instances of such local peak negative accelerations in the x-axis indicate the start instance of the recovery phase of each stroke. Similarly, a high resultant acceleration a_{res} calculated using equation 2 indicates the start of a propulsion phase, as wheelchair users usually increase hand acceleration before the propulsion phase and control the acceleration during the propulsion phase in order for the hand to follow the pushrim. The program first detected the maximum resultant acceleration and created a band of 50% to 100% of the maximum value to detect other local peak resultant accelerations. The instances of such local peak resultant accelerations indicate the start instance of the propulsion phase of each stroke. Figure 2 shows an example of the acceleration signals (a_x and a_{res}) compared with the recovery and propulsion phases identified by the SMART^{Wheel} over three consecutive strokes.

Figure 2 and Equation 2 Go Here

Based on the time instances of each propulsion and recovery phase, the temporal parameters of wheelchair propulsion including propulsion time, recovery time, and stroke frequency were obtained based on both the hand acceleration and the reference SMART^{Wheel}.

Statistical Analysis: Intraclass correlations (ICCs) were used to assess agreement between the two methods. ICC(3,1) for single measure using two-way mixed model with consistency were performed on the propulsion time, recovery time, and stroke time over level linoleum and carpet surfaces. An ICC value of ≥ 0.75 is considered good and ≥ 0.9 is deemed excellent (7). The level of agreement between the two methods for the start instances of propulsion and recovery phases over the surfaces were also examined graphically using the Bland and Altman method (8).

RESULTS

Twenty-nine manual wheelchair users consisting of twenty-eight men and one woman provided the informed consent and took part in the study. The average age of the subject population was 46.7 ± 9.7 years and the average period post injury was 14.2 ± 9.9 years. Twenty-four subjects had spinal cord injury with varied levels, 3 had amputations, 1 had peripheral neuropathy, and 1 had spina bifida at L4.

Table 1 shows the average temporal parameters of propulsion strokes determined by hand acceleration and the SMART^{Wheel}. The ICCs of the stroke time, propulsion time, and recovery time were 0.938, 0.815, 0.753 on the tile surface and 0.994, 0.962, 0.901 on the carpet surface, respectively (Table 2). The Bland and Altman plots for the start instances of propulsion and recovery phases determined by the two methods are presented in Figure 3 and Figure 4, respectively. The difference between the mean of the two methods for the start instances of propulsion and recovery phases were 0.037s and 0.023s, respectively. For both phases, more than 95% of the estimated values lie within Mean ± 2SD (standard deviation) of the SMART^{Wheel} values.

Table 1, 2 Goes Here

Figure 3, 4 Goes Here

DISCUSSION

The purpose of this study was to verify if the temporal parameters of wheelchair propulsion can be reliably and accurately estimated by hand acceleration signals. The SMART^{Wheel} was selected as reference criteria as it is generally used to measure propulsion biomechanics in laboratories settings and has shown to exhibit excellent linearity and accuracy (9). Our study showed that the local peaks in a_x and a_{res} closely matched the start instances of recovery and propulsion phases detected by the SMART^{Wheel} (Figure 2). The high ICC values also indicate strong agreement between the estimated temporal parameters and reference criteria. The ICC values for the carpet trials were higher than the linoleum trials with the lower limits of the 95% confidence interval of the ICCs exceeding 0.75 for all three temporal parameters (7). The reason could be that the number of strokes per trial was higher on carpet due to higher rolling resistance, and more strokes were captured by the system compared to linoleum. The lesser ICC values for the recovery time could be caused by different propulsion patterns and traveling speeds between subjects (10). The method of utilizing only start instances of propulsion phases to calculate the stroke time resulted in less variation and very high ICC values on both surfaces. The Bland and Altman plots (Figure 3 and 4) showed that the mean differences were close to zero and more than 95% of the values lie within

Mean ± 2SD, indicating excellent agreement between the two methods for determining the start instances of propulsion and recovery phases.

Inability of the vision system to capture more strokes per trial was a limitation to the study. There were four trials on the carpet and three trials on linoleum where the values of a_x did not fall in the band selected by the algorithm and the detection failed. Longer trials with more strokes and examination of the history local peak accelerations for band parameter optimization could be investigated to enhance the detection accuracy of recovery and propulsion phases in the future. Future work will also investigate the relationship between hand acceleration and other biomechanical variables such as propulsion forces, and conduct experiments with accelerometer-based activity monitors to further verify the algorithms.

The reliable and accurate detection of stroke phases via hand acceleration when wheelchair users propel at their own paces on natural surfaces indicates great potential for future research. The algorithm could be incorporated in devices like activity monitors which could be worn on the wrist to indicate propulsion performance. Activity monitors that can measure stroke frequency in the natural environment of wheelchair users may help researchers and clinicians to quantify propulsion performance and upper limb usage, and monitor the effectiveness of the interventions during propulsion training.

REFERENCE

1. Frost P., Bonde J. P., Mikkelsen S., et al. (2002). Risk of shoulder tendinitis in relation to shoulder loads in monotonous repetitive work. American Journal of Industrial Medicine. 41:11-18.
2. Roquelaure Y., Mechali S., Dano C., et al (1997). Occupational and personal risk factors for carpal tunnel syndrome in industrial workers. Scandinavian Journal of Work, Environment & Health. 23:364-369.
3. Bonninger M. L., Koontz A. M., Sisto S. A., Dyson-Hudson T. A., Chang M., Price R. et al. (2005). Pushrim biomechanics and injury prevention in spinal cord injury: recommendations based on CULP-SCI investigations. Journal of Rehabilitation Research & Development. 42(3):9-20.
4. Postma K., van den Berg-Emons H. J., Bussmann J. B., Sluis T. A., Bergen M. P., Stam H. J. (2005). Validity of the detection of wheelchair propulsion as measured with an activity monitor in patients with spinal cord injury. Spinal Cord. 43(9):550-7.
5. Jungh-Ah L., Sang-Hyu C., Jeong-Whan L., Kang-Hwi L., Heui-Kyung Y. (2007). Wearable accelerometer systems for measuring the temporal parameters of gait. 29th Annual International Conference of the IEEE EMBS.
6. Winter D. A. (1990). Biomechanics and motor control of human movement (2nd ed.). Published by John Wiley & Sons, New York.
7. Lee J., Koh D., Ong C. N. (1989). Statistical evaluation of agreement between two methods for measuring the same quantity. Computers in Biology and Medicine. 19(1):61–70.
8. Bland J. M., Altman D. G. (1986). Statistical methods for assessing agreement between two methods of clinical measurement. Lancet 1:307-10.
9. Asato K. T., Cooper R. A., Robertson R. N., Ster J. F. (1993). SmartWheels: Development and Testing of a System for Measuring Manual Wheelchair Propulsion Dynamics. IEEE Trans Biomed Eng. 40 (12) 1320-4.
10. Roche B., Koontz A., Yarnall M., Mercer J., Cowan R., Boninger M. (2007). Manual wheelchair propulsion patterns on natural surfaces. RESNA Annual Conference.

ACKNOWLEDGEMENTS

The work is supported by PVA#2486, and VA Center of Excellence for Wheelchairs and Associated Rehabilitation Engineering B3142C.

Shivayogi Hiremath, Human Engineering Research Laboratories, 7180 Highland Dr., 151R1-H, Pittsburgh, PA 15206. 412-365-5561. svh4@pitt.edu.

GRAPHICS PAGE

Figure 1: The two-dimensional hand (3MP) position plots of three consecutive propulsion strokes from one of the subjects.

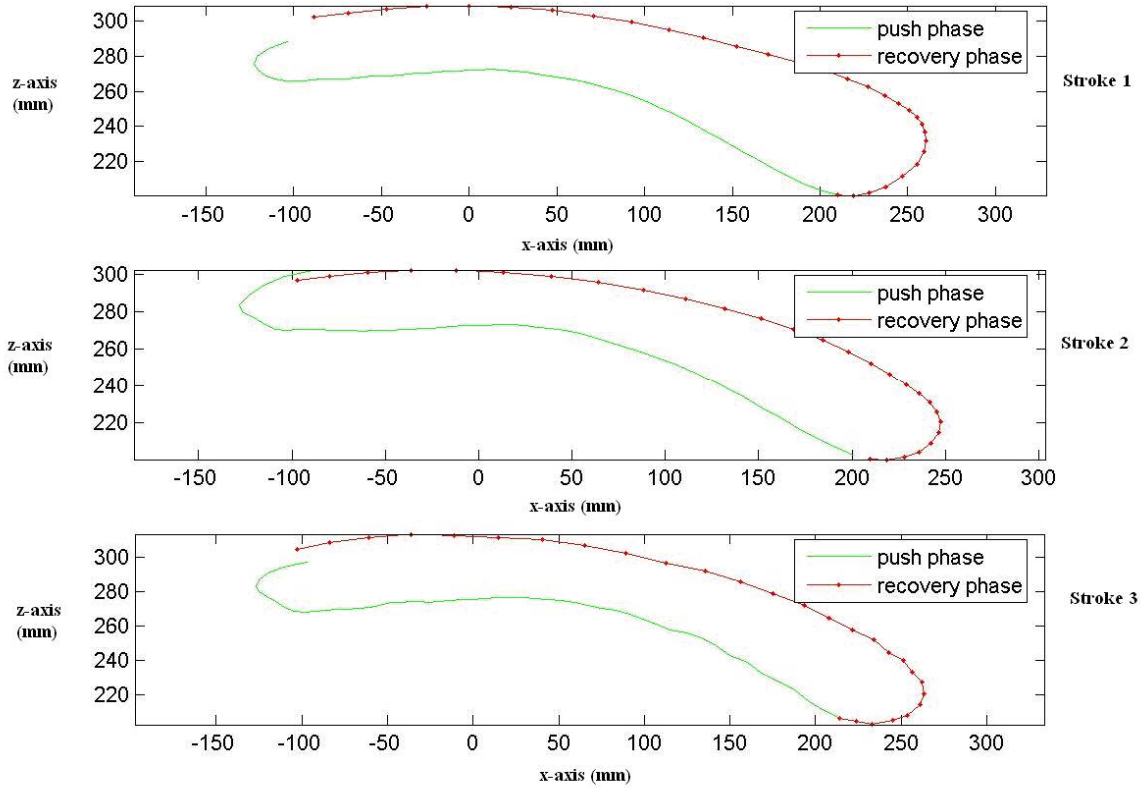

Alternative Text Description for Figure 1:
The plots indicate the motion of the hand in the direction of wheelchair motion (x-axis) and against gravity (z-axis), for three consecutive propulsion strokes.

Figure 2: The acceleration signals (a_x and a_{res}) and the recovery and propulsion phases identified by the SMART^{Wheel} over three consecutive strokes shown in Figure 1.

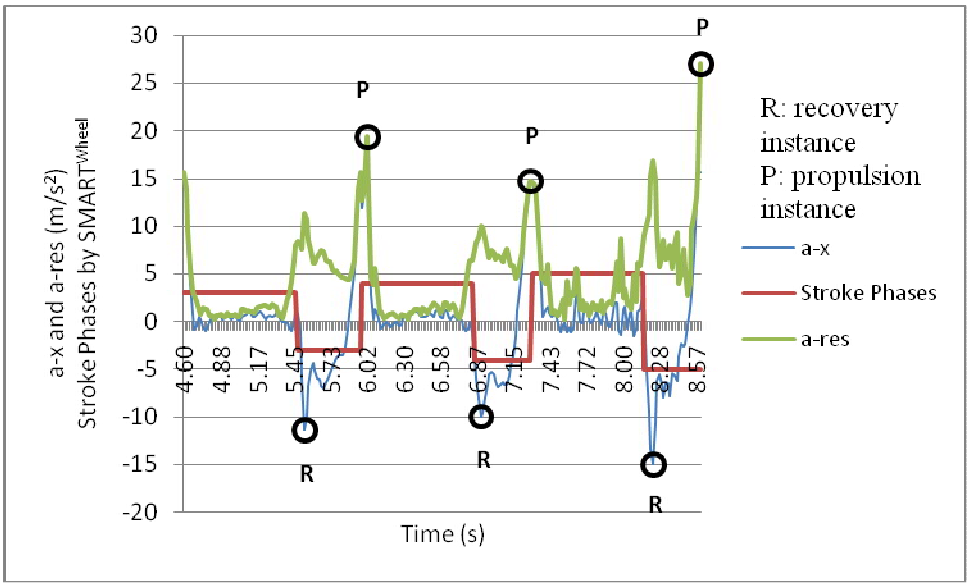

Alternative Text Description for Figure 2:

P indicates positive resultant acceleration peak, detected by the estimation algorithm as the start instance of propulsion phase. R indicates negative acceleration in x direction, detected by the estimation algorithm as the start instance of recovery phase. Stroke phase indicates the propulsion and recovery phases as detected by the SMART^{Wheel}.

Figure 3: The Bland and Altman plot for the start instances of recovery phases on carpet determined by hand acceleration and the SMART^{Wheel}. Similar plot was obtained for the data on tile surface.

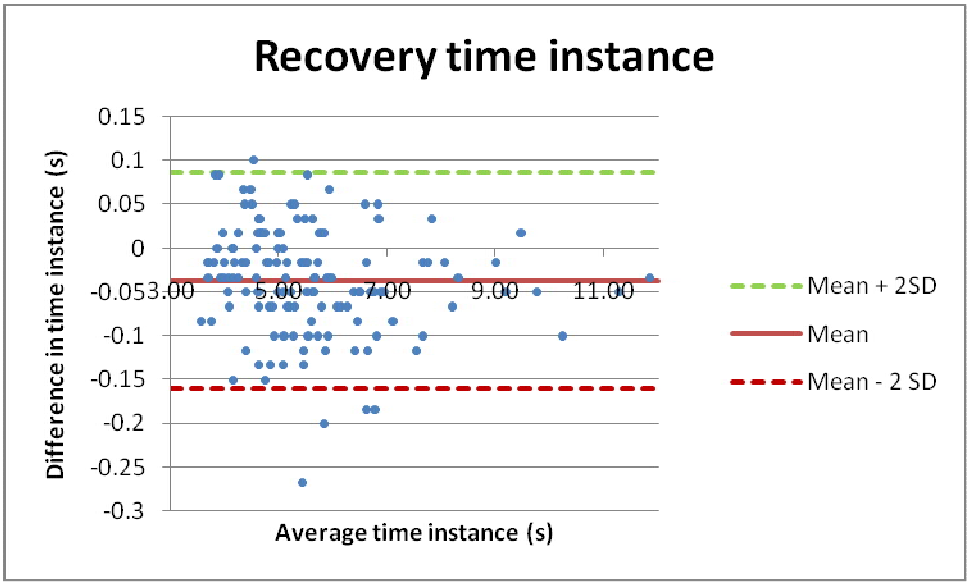

Alternative Text Description for Figure 3:

Only five out of one hundred and thirty strokes on the carpet lie outside the mean $\pm$ 2 standard deviation indicating more than 95% of the predicted values agree with the measured value.

Figure 4: The Bland and Altman plots for the start instances of propulsion phases on carpet determined by hand acceleration and the SMART^{Wheel}. Similar plot was obtained for tile surface.

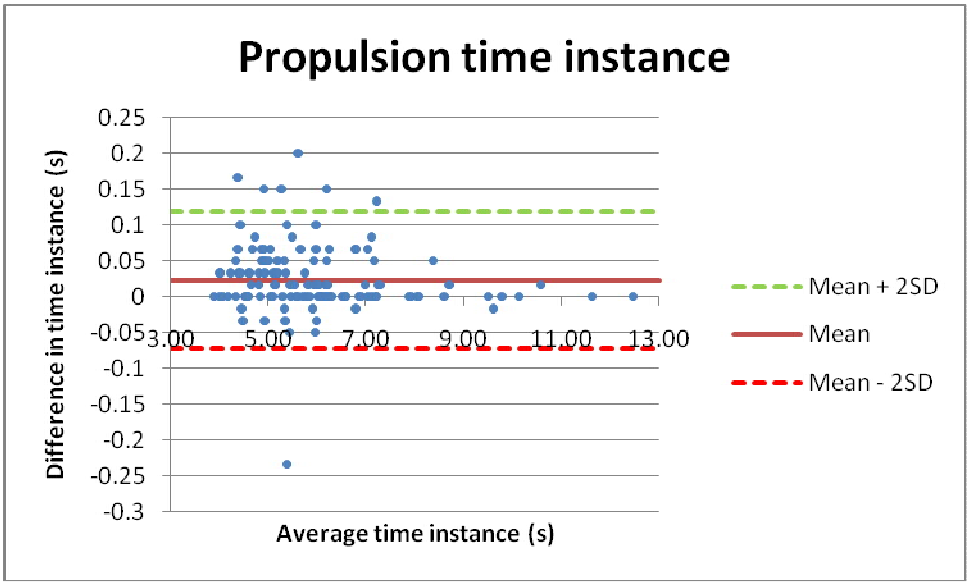

Alternative Text Description for Figure 4:
Only seven out of one hundred and thirty strokes on carpet lie outside the mean $\pm$ 2 standard deviation indicating more than 95% of the predicted values agree with the measured value.

Table 1: Average temporal parameters of propulsion strokes determined by hand acceleration and the SMART^{Wheel}.

	Estimates of temporal parameters based on hand acceleration (s)			Reference temporal parameters based on the SMART^{Wheel} (s)		
	Stroke Time Mean (SD)	Propulsion Time Mean (SD)	Recovery Time Mean (SD)	Stroke Time Mean (SD)	Propulsion Time Mean (SD)	Recovery Time Mean (SD)
Tile	0.94(0.20)	0.60 (0.11)	0.45 (0.08)	0.94 (0.23)	0.53 (0.13)	0.53 (0.09)
Carpet	1.07 (0.23)	0.70 (0.18)	0.38 (0.08)	1.07 (0.23)	0.64 (0.17)	0.44 (0.07)

Alternative Text Description for Table 1:
This table averages all the stroke times, propulsion times and recovery times for all the strokes on tile and carpet surface.

Table 2: Intraclass correlation coefficients ICC(3,1) for temporal parameters of wheelchair propulsion based on hand acceleration and SMART^{Wheel} on tile and carpet surfaces

---

Surface	Temporal parameters	ICC(3,k)	95% confidence interval	p (significance)
Tile	Stroke Time	0.938	0.772~0.984	0.000
	Propulsion Time	0.815	0.450~0.947	0.006
	Recovery Time	0.753	0.440~0.930	0.002
Carpet	Stroke Time	0.994	0.984~0.998	0.000
	Propulsion Time	0.962	0.898~0.986	0.000
	Recovery Time	0.901	0.782~0.957	0.000

Alternative Text Description for Table 2:
High values indicate the reliability and the agreement of the two methods with good significance, $p<0.01$.

Equation 1:

$$v_x(i+1) = \frac{(x(i+2) - x(i))}{2 * \Delta t}$$

$$a_x(i+1) = \frac{(v_x(i+2) - v_x(i))}{2 * \Delta t}$$

Alternative Text Description for Equation 1:
$v_x(i+1)$ (m/s) is the instantaneous velocity in the x-direction at the time instance, *i+1*. *x(i)* and *x(i+2)* are the positions of the point in the x-axis at time instances of *i* and *i*+2. $a_x(i+1)$ (m/s^2) is the instantaneous acceleration in the x-direction at the time instance, *i*+1. $v_x(i)$ and $v_x(i+2)$ are the velocities of the point in the x-axis at time instances of *i* and *i*+2. Δt is the time difference between two instances of the position (here it is 1/60 Hz as the capture rate of vision system is 60 Hz).

Equation 2:

$$a_{res}(i) = \sqrt{(a_x^2(i) + a_y^2(i) + a_z^2(i))}$$

Alternative Text Description for Equation 2:
$a_{res}(i)$ (m/s^2) is the resultant acceleration in the x-direction at the time instance, *i*. $a_x(i)$, $a_y(i)$ $a_z(i)$ are the instantaneous accelerations of the point in the x-axis, y-axis and z-axis at time instance *i*.